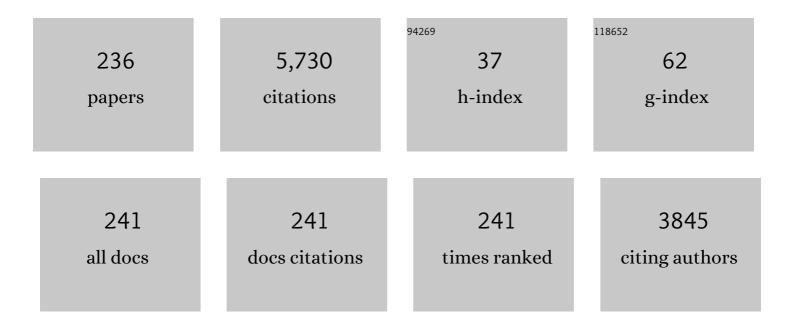
## Iftikhar Ahmad

List of Publications by Year in descending order

Source: https://exaly.com/author-pdf/4490904/publications.pdf Version: 2024-02-01



#	Article	IF	CITATIONS
1	Elastic constants of cubic crystals. Computational Materials Science, 2014, 95, 592-599.	1.4	341
2	First principle study of the structural and optoelectronic properties of cubic perovskites CsPbM3 (M=Cl, Br, l). Physica B: Condensed Matter, 2011, 406, 3222-3229.	1.3	263
3	Structural, electronic and optical properties of CsPbX3 (X=Cl, Br, I) for energy storage and hybrid solar cell applications. Journal of Alloys and Compounds, 2017, 705, 828-839.	2.8	203
4	IRelast package. Journal of Alloys and Compounds, 2018, 735, 569-579.	2.8	198
5	<i>Ab initio</i> study of the bandgap engineering of Al1â <sup>~</sup> 'xGaxN for optoelectronic applications. Journal of Applied Physics, 2011, 109, .	1.1	167
6	Rashba spin splitting and photocatalytic properties of <mml:math xmlns:mml="http://www.w3.org/1998/Math/MathML"&gt;<mml:mi>GeC</mml:mi><mml:mo>â^'</mml:mo><mml:rr ( <mml:math) (xmlns:mml="http://www.w3.org/1998/Math/MathMl&lt;/td&gt;&lt;td&gt;ni&gt;M&lt;/mm&lt;br&gt;_" 0="" 10="" 50="" 537="" atamml:n<="" etqq0="" overlock="" rgbt="" td="" tf="" tj=""><td>l:mi&gt;<mml:m nr<b>o4v</b>4&gt;<mml:< td=""></mml:<></mml:m </td></mml:math)></mml:rr </mml:math 	l:mi> <mml:m nr<b>o4v</b>4&gt;<mml:< td=""></mml:<></mml:m 	
7	Optoelectronic and solar cell applications of Janus monolayers and their van der Waals heterostructures. Physical Chemistry Chemical Physics, 2019, 21, 18612-18621.	1.3	141
8	Investigation of structural and optoelectronic properties of BaThO3. Optical Materials, 2011, 33, 553-557.	1.7	124
9	Ab initio calculations of structural, optical and thermoelectric properties for CoSb3 and ACo4Sb12 (A=La, Tl and Y) compounds. Computational Materials Science, 2012, 65, 509-519.	1.4	95
10	Electronic structure, optical and photocatalytic performance of SiC–MX <sub>2</sub> (M = Mo, W) Tj ETQq0 ( 24168-24175.	) 0 rgBT /C 1.3	)verlock 10 T 85
11	On the Morphology and Composition of Particulate Matter in an Urban Environment. Aerosol and Air Quality Research, 2018, 18, 1431-1447.	0.9	81
12	Direct ultraviolet excitation of an amorphous AlN:praseodymium phosphor by codoped Gd3+ cathodoluminescence. Applied Physics Letters, 2007, 91, .	1.5	75
13	Intriguing electronic structures and optical properties of two-dimensional van der Waals heterostructures of Zr <sub>2</sub> CT <sub>2</sub> (T = O, F) with MoSe <sub>2</sub> and WSe <sub>2</sub> . Journal of Materials Chemistry C, 2018, 6, 2830-2839.	2.7	73
14	Thermoelectric properties of SbNCa3 and BiNCa3 for thermoelectric devices and alternative energy applications. Computer Physics Communications, 2014, 185, 1394-1398.	3.0	70
15	Morphological, Raman, electrical and dielectric properties of rare earth doped X-type hexagonal ferrites. Physica B: Condensed Matter, 2016, 503, 38-43.	1.3	60
16	Strain engineering of electronic structures and photocatalytic responses of MXenes functionalized by oxygen. Physical Chemistry Chemical Physics, 2017, 19, 14738-14744.	1.3	60
17	First principle studies of structural, elastic, electronic and optical properties of Zn-chalcogenides under pressure. Journal of Semiconductors, 2014, 35, 072001.	2.0	58
18	Thermoelectric studies of IV–VI semiconductors for renewable energy resources. Materials Science in Semiconductor Processing, 2016, 48, 85-94.	1.9	58

#	Article	IF	CITATIONS
19	Opto-electronic response of spinels MgAl2O4 and MgGa2O4 through modified Becke-Johnson exchange potential. Physica B: Condensed Matter, 2012, 407, 2588-2592.	1.3	57
20	Van der Waals heterostructures of P, BSe, and SiC monolayers. Journal of Applied Physics, 2019, 125, .	1.1	57
21	Electronic structure of cubic perovskite SnTaO3. Intermetallics, 2012, 31, 287-291.	1.8	55
22	Electronic Band Structures of the Highly Desirable III–V Semiconductors: TB-mBJ DFT Studies. Journal of Electronic Materials, 2016, 45, 3314-3323.	1.0	54
23	Conversion of Direct to Indirect Bandgap and Optical Response of B Substituted InN for Novel Optical Devices Applications. Journal of Lightwave Technology, 2010, 28, 223-227.	2.7	53
24	Theoretical studies of structural and magnetic properties of cubic perovskites PrCoO3 and NdCoO3. Physica B: Condensed Matter, 2011, 406, 3800-3804.	1.3	48
25	Shift of indirect to direct bandgap and optical response of LaAlO3 under pressure. Journal of Applied Physics, 2012, 111, .	1.1	48
26	Conversion of optically isotropic to anisotropic CdSxSe1â^'x (0⩽x⩽1) alloy with S concentration. Computational Materials Science, 2013, 77, 145-152.	1.4	48
27	Structural and Optoelectronic Properties of Cubic CsPbF <sub>3</sub> for Novel Applications. Chinese Physics Letters, 2011, 28, 117803.	1.3	45
28	First principle study of cubic perovskites: AgTF3 (T=Mg, Zn). Physica B: Condensed Matter, 2011, 406, 4584-4589.	1.3	45
29	Effect of phase transition on the optoelectronic properties of Zn1â^'xMgxS. Journal of Applied Physics, 2012, 112, .	1.1	45
30	Structural and optoelectronic properties of the zinc titanate perovskite and spinel by modified Becke–Johnson potential. Physica B: Condensed Matter, 2013, 420, 54-57.	1.3	44
31	Cr-Doped Ill–V Nitrides: Potential Candidates for Spintronics. Journal of Electronic Materials, 2011, 40, 1428-1436.	1.0	43
32	Metal mono-chalcogenides ZnX and CdX (X = S, Se and Te) monolayers: Chemical bond and optical interband transitions by first principles calculations. Physics Letters, Section A: General, Atomic and Solid State Physics, 2017, 381, 663-670.	0.9	43
33	Electronic and optical properties of mixed Be-chalcogenides. Journal of Physics and Chemistry of Solids, 2013, 74, 181-188.	1.9	42
34	GGA+U studies of the cubic perovskites BaMO3 (M=Pr, Th and U). Physica B: Condensed Matter, 2013, 410, 217-221.	1.3	41
35	Gray-box modeling for prediction and control of molten steel temperature in tundish. Journal of Process Control, 2014, 24, 375-382.	1.7	40
36	Antiperovskite compounds SbNSr3 and BiNSr3: Potential candidates for thermoelectric renewable energy generators. Physics Letters, Section A: General, Atomic and Solid State Physics, 2015, 379, 206-210.	0.9	40

#	Article	IF	CITATIONS
37	First-principles study of BiFeO <sub>3</sub> and BaTiO <sub>3</sub> in tetragonal structure. International Journal of Modern Physics B, 2019, 33, 1950231.	1.0	40
38	Theoretical studies of the paramagnetic perovskites MTaO3 (MÂ=ÂCa, Sr and Ba). Materials Chemistry and Physics, 2015, 162, 308-315.	2.0	38
39	Bandgap investigations and the effect of the In and Al concentration on the optical properties of In_xAl_1â°'xN. Journal of the Optical Society of America B: Optical Physics, 2009, 26, 2181.	0.9	37
40	Robust half-metallicity in Ga1-xMnxP and Ga1-xMnxAs. Computational Materials Science, 2013, 68, 55-60.	1.4	37
41	van der Waals heterostructures based on MSSe (M = Mo, W) and graphene-like GaN: enhanced optoelectronic and photocatalytic properties for water splitting. Physical Chemistry Chemical Physics, 2020, 22, 20704-20711.	1.3	37
42	Theoretical investigation of half metallicity in Fe/Co/Ni doped ZnSe material systems. Journal of Applied Physics, 2009, 106, .	1.1	36
43	Theoretical studies of strongly correlated rare-earth intermetallics RIn3 and RSn3 (R = Sm, Eu, and Gd). Journal of Applied Physics, 2014, 116, .	1.1	36
44	Theoretical investigation of electronic structure and thermoelectric properties of MX2 (M=Zr, Hf;) Tj ETQq0 0 0 $r_{ m s}$	gBT /Overl 1.9	ock 10 Tf 50
45	Shift of indirect to direct bandgap in going from K to Cs in MCaF3 (MÂ=ÂK, Rb, Cs). Solid State Sciences, 2013, 16, 152-157.	1.5	35
46	Bandgap engineering of Cd1â^'xSrxO. Physica B: Condensed Matter, 2011, 406, 2509-2514.	1.3	33
47	Elastic and Optoelectronic Properties of Cs2NaMCl6 (M = In, Tl, Sb, Bi). Journal of Electronic Materials, 2021, 50, 456-466.	1.0	33
48	Structural, electronic and optical properties of CaxCd1â°'xO and its conversion from semimetal to wide bandgap semiconductor. Computational Materials Science, 2012, 58, 71-76.	1.4	32
49	Electronic Properties of Antiperovskite Materials from State-of-the-Art Density Functional Theory. Journal of Chemistry, 2015, 2015, 1-11.	0.9	32
50	Structural and optoelectronic properties of Mg substituted ZTe (Z=Zn, Cd and Hg). Journal of Physics and Chemistry of Solids, 2015, 83, 75-84.	1.9	32
51	Elastic and mechanical properties of lanthanide monoxides. Journal of Alloys and Compounds, 2015, 618, 292-298.	2.8	32
52	Structural, microwave permittivity, and complex impedance studies of cation (Cr, Bi, Al, In) substituted SrNi-X hexagonal nano-sized ferrites. Ceramics International, 2020, 46, 1907-1915.	2.3	32
53	Removal of azo dye from aqueous solution by a low-cost activated carbon prepared from coal: adsorption kinetics, isotherms study, and DFT simulation. Environmental Science and Pollution Research, 2021, 28, 10234-10247.	2.7	30
54	Silicon carbide and III-Nitrides nanosheets: Promising anodes for Mg-ion batteries. Materials Chemistry and Physics, 2021, 257, 123785.	2.0	29

#	Article	IF	CITATIONS
55	Gray-box Soft Sensors in Process Industry: Current Practice, and Future Prospects in Era of Big Data. Processes, 2020, 8, 243.	1.3	28
56	Influence of electric field on CO2 removal by P-doped C60-fullerene: A DFT study. Chemical Physics Letters, 2020, 742, 137155.	1.2	28
57	Transition from optically inactive to active Mg-chalcogenides: A first principle study. Computational Materials Science, 2012, 61, 278-282.	1.4	27
58	Investigation of half metallicity in Fe doped CdSe and Co doped CdSe materials. Current Applied Physics, 2012, 12, 184-187.	1.1	27
59	Band Profile Comparison of the Cubic Perovskites CaCoO3 and SrCoO3. Journal of Electronic Materials, 2013, 42, 438-444.	1.0	27
60	Structural and thermoelectric properties of pure and La, Y doped HoMnO3 for their use as alternative energy materials. Computer Physics Communications, 2015, 187, 1-7.	3.0	27
61	Thermoelectric and phononic properties of (Gd, Tb) MnO3 compounds: DFT calculations. Journal of Alloys and Compounds, 2017, 690, 942-952.	2.8	27
62	Electronic Structure of Crystalline Buckyballs: fcc-C60. Journal of Electronic Materials, 2016, 45, 339-348.	1.0	26
63	Effects of cobalt substitution on the physical properties of the perovskite strontium ferrite. Materials Chemistry and Physics, 2017, 196, 222-228.	2.0	26
64	Linear and nonlinear optical response of MgxZn1â^'xO: A density functional study. Physica B: Condensed Matter, 2011, 406, 2632-2636.	1.3	25
65	The investigation of spherical effects on the photodetached electron spectra. Journal of Physics B: Atomic, Molecular and Optical Physics, 2011, 44, 195004.	0.6	25
66	Theoretical studies of the band structure and optoelectronic properties of ZnO <sub><i>x</i></sub> S <sub>1â^'<i>x</i></sub> . International Journal of Quantum Chemistry, 2013, 113, 1285-1292.	1.0	25
67	Density functional theory study of emerging pollutants removal from water by covalent triazine based framework. Journal of Molecular Liquids, 2020, 309, 113008.	2.3	25
68	Generalized gradient calculations of structural, electronic and optical properties of MgxCd1â^'xO oxides. Journal of Alloys and Compounds, 2010, 493, 212-218.	2.8	24
69	Structural, optical, and electrical characteristics of AlN:Ho thin films irradiated with 700 keV protons. Applied Surface Science, 2015, 357, 179-183.	3.1	24
70	Influence of Cr and Zn substitution on structural, magnetic and dielectric properties of Sr2-xZnxNi2Fe28-yCryO46 X-type hexagonal ferrite. Solid State Sciences, 2020, 100, 106090.	1.5	24
71	First-Principles Study of Perovskite Molybdates AMoO3 (A = Ca, Sr, Ba). Journal of Electronic Materials, 2019, 48, 1730-1739.	1.0	23
72	Theoretical studies of the osmium based perovskites AOsO3 (A=Ca, Sr and Ba). Journal of Physics and Chemistry of Solids, 2015, 86, 114-121.	1.9	22

5

#	Article	IF	CITATIONS
73	First principle study of band gap nature, spontaneous polarization, hyperfine field and electric field gradient of desirable multiferroic bismuth ferrite (BiFeO3). Journal of Physics and Chemistry of Solids, 2021, 148, 109737.	1.9	22
74	Synthesis, characterization, and biological study of some biologically potent schiff base transition metal complexes. Russian Journal of Coordination Chemistry/Koordinatsionnaya Khimiya, 2008, 34, 678-682.	0.3	21
75	Detailed DFT studies of the band profiles and optical properties of antiperovskites SbNCa3 and BiNCa3. Computational Materials Science, 2014, 85, 310-315.	1.4	21
76	Electronic structure and magnetic properties of the perovskites SrTMO3 (TM = Mn, Fe, Co, Tc, Ru, Rh,) Tj ETQq0 (	0 o rgBT /0 1.3	Verlock 10 T
77	Coherent control of polarization state rotation via Doppler broadening and Kerr nonlinearity in a spinning fast light medium. Laser Physics, 2014, 24, 115404.	0.6	20
78	Effect of strain on structural and electronic properties, and thermoelectric response of MXY (M=Zr,) Tj ETQq0 0 0 2021, 299, 122189.	rgBT /Ove 1.4	erlock 10 Tf 5 20
79	Optoelectronic properties of KDP by first principle calculations. International Journal of Quantum Chemistry, 2013, 113, 865-872.	1.0	19
80	Thermoelectric properties of metallic antiperovskites AXD3 (A=Ge, Sn, Pb, Al, Zn, Ga; X=N, C; D=Ca, Fe,) Tj ETQq0	0.0 rgBT 1.0	Overlock 10

81	GaN–MX <sub>2</sub> (M = Mo, W; X= S, Se) van der Waals heterostructures. RSC Advances, 2020, 10, 24683-24690.	1.7	19
82	Effects of Ni Substitution on the Electronic Structure and Magnetic Properties of Perovskite SrFeO3. Journal of Electronic Materials, 2020, 49, 3780-3790.	1.0	19
83	In-Depth Analysis of Physicochemical Properties of Particulate Matter (PM10, PM2.5 and PM1) and Its Characterization through FTIR, XRD and SEM–EDX Techniques in the Foothills of the Hindu Kush Region of Northern Pakistan. Atmosphere, 2022, 13, 124.	1.0	19
84	Gain assisted multiple surperluminal regions via a Kerr nonlinearity in a double lambda-type atomic configuration. Laser Physics, 2014, 24, 055401.	0.6	18
85	First-principle studies of the optoelectronic properties of ASnF <sub>3</sub> (A = Na, K, Rb and Cs). International Journal of Modern Physics B, 2017, 31, 1750148.	1.0	18
86	Tunable relativistic quasiparticle electronic and excitonic behavior of the FAPb(I <sub>1â^²x</sub> Br <sub>x</sub> ) <sub>3</sub> alloy. Physical Chemistry Chemical Physics, 2020, 22, 11943-11955.	1.3	18
87	Selective adsorption of CO2 from gas mixture by P-decorated C24N24 fullerene assisted by an electric field: A DFT approach. Journal of Molecular Graphics and Modelling, 2021, 103, 107806.	1.3	18
88	Optoelectronic Response of GeZn <sub>2</sub> O <sub>4</sub> through the Modified Becke—Johnson Potential. Chinese Physics Letters, 2012, 29, 097102.	1.3	17
89	DFT-mBJ Studies of the Band Structures of the II-VI Semiconductors. Materials Today: Proceedings, 2015, 2, 5122-5127.	0.9	17
90	Tunable surface plasmon polaritons at the surfaces of nanocomposite media. Europhysics Letters, 2018, 122, 17001.	0.7	17

#	Article	IF	CITATIONS
91	Structural features and dielectric behavior of Al substituted Cu0.7Ni0.3Fe2O4 ferrites. Materials Chemistry and Physics, 2021, 273, 125028.	2.0	17
92	Optoelectronic properties of LixAxNbO3 (A=Na, K, Rb, Cs, Fr) crystals. Physica B: Condensed Matter, 2012, 407, 368-377.	1.3	16
93	Structural and magnetic properties of TITF3 (T=Fe, Co and Ni) by hybrid functional theory. Journal of Magnetism and Magnetic Materials, 2015, 388, 143-149.	1.0	16
94	Temporal characteristics of aerosol optical properties over the glacier region of northern Pakistan. Journal of Atmospheric and Solar-Terrestrial Physics, 2019, 186, 35-46.	0.6	16
95	Theoretical Investigations of Quaternary Semiconductors CsInCdTe3 (Ln = La, Pr, Nd and Sm). Journal of Electronic Materials, 2020, 49, 3357-3366.	1.0	16
96	Theoretical investigation of halfâ€metallicity in Co/Ni substituted AlN. International Journal of Quantum Chemistry, 2012, 112, 882-888.	1.0	15
97	Robust Half-Metallicity and Magnetic Properties of Cubic Perovskite CaFeO 3. Chinese Physics Letters, 2013, 30, 047504.	1.3	15
98	First principle optoelectronic studies of visible light sensitive CZT. Superlattices and Microstructures, 2013, 63, 91-99.	1.4	15
99	Comparison of the electronic band profiles and magneto-optic properties of cubic and orthorhombic SrTbO3. Physica B: Condensed Matter, 2013, 423, 16-20.	1.3	15
100	Control of Group Velocity via Spontaneous Generated Coherence and Kerr Nonlinearity. Communications in Theoretical Physics, 2014, 62, 410-416.	1.1	15
101	Ab initio studies of electric field gradients and magnetic properties of uranium dipnicties. RSC Advances, 2015, 5, 37592-37602.	1.7	15
102	Role of nitrogen vacancies in cerium doped aluminum nitride. Journal of Magnetism and Magnetic Materials, 2016, 412, 49-54.	1.0	15
103	Strain engineering of Janus ZrSSe and HfSSe monolayers and ZrSSe/HfSSe van der Waals heterostructure. Chemical Physics Letters, 2021, 776, 138689.	1.2	15
104	Electronic structure, optical and magnetic properties of double Perovskites La2MTiO6 (M = Co, Ni, Cu) Tj ETQq0 0	9.rgBT /O	verlock 10 <sup>-</sup> 15
105	Penta graphene: a superior anode material for Mg-ion batteries with high specific theoretical capacity. Ionics, 2021, 27, 4819-4828.	1.2	15
106	Photodetachment of H â^' near a Hard Spherical Surface. Chinese Physics Letters, 2012, 29, 013202.	1.3	14
107	High-Performance Prediction of Molten Steel Temperature in Tundish through Gray-Box Model. ISIJ International, 2013, 53, 76-80.	0.6	14

<sup>108</sup>Magneto-electronic studies of anti-perovskites NiNMn3 and ZnNMn3. Computational Materials Science,<br/>2014, 81, 141-145.1.414

#	Article	IF	CITATIONS
109	Effects of dangling bonds and diameter on the electronic and optical properties of InAs nanowires. RSC Advances, 2015, 5, 23320-23325.	1.7	14
110	Pressure dependency of localization degree in heavy fermion Celn3: A density functional theory analysis. Scientific Reports, 2016, 6, 31734.	1.6	14
111	Van der Waals heterostructures of blue phosphorene and scandium-based MXenes monolayers. Journal of Applied Physics, 2019, 126, .	1.1	14
112	Effects of A-Site cation on the Physical Properties of Quaternary Perovskites AMn3V4O12 (A= Ca, Ce) Tj ETQq0 0	0.rgBT /Ov 2.0	verlock 10 Tr 14
113	Black Carbon aerosol characteristics and radiative forcing over the high altitude glacier region of Himalaya-Karakorum-Hindukush. Atmospheric Environment, 2020, 238, 117711.	1.9	14
114	Effect of size reduction on the electronic and ferromagnetic properties of the In2O3 nanoparticles. Journal of Nanoparticle Research, 2012, 14, 1.	0.8	13
115	Prediction of Molten Steel Temperature in Steel Making Process with Uncertainty by Integrating Gray-Box Model and Bootstrap Filter. Journal of Chemical Engineering of Japan, 2014, 47, 827-834.	0.3	13
116	Optical properties of ideal γ-Al <sub>2</sub> O <sub>3</sub> and with oxygen point defects: an ab initio study. RSC Advances, 2015, 5, 55088-55099.	1.7	13
117	Energy level splitting and luminescence enhancement in AlN:Er by an external magnetic field. Optical Materials, 2015, 46, 601-604.	1.7	13
118	Electronic band structures of binary skutterudites. Journal of Alloys and Compounds, 2015, 647, 364-369.	2.8	13
119	First-principles study of structural, electronic, magnetic and thermoelectric properties of the cubic mono-pnictides of thorium Th Pn ( Pn = Sb and Bi). Computational Condensed Matter, 2017, 13, 111-119.	0.9	13
120	First principle studies of electronic and magnetic properties of Lanthanide-Gold (RAu) binary intermetallics. Journal of Magnetism and Magnetic Materials, 2017, 422, 458-463.	1.0	13
121	Dimensions and Analysis of Uncertainty in Industrial Modeling Process. Journal of Chemical Engineering of Japan, 2018, 51, 533-543.	0.3	13
122	Intriguing electronic and optical properties of M2CX2 (M = Mo, W; X = O, F) MXenes and their van der Waals heterostructures. Chemical Physics Letters, 2019, 731, 136614.	1.2	13
123	Nanocrystals formation and intense green emission in thermally annealed AlN:Ho films for microlaser cavities and photonic applications. Journal of Applied Physics, 2010, 108, .	1.1	12
124	Quasiparticle optoelectronic properties of pure and doped indium oxide. Optical Materials, 2012, 34, 1406-1414.	1.7	12
125	Deep ultraviolet photopumped stimulated emission from partially relaxed AlGaN multiple quantum well heterostructures grown on sapphire substrates. Journal of Vacuum Science and Technology B:Nanotechnology and Microelectronics, 2014, 32, .	0.6	12
126	Control of slow-to-fast light and single-to-double optomechanically induced transparency in a compound resonator system: A theoretical approach. Europhysics Letters, 2017, 120, 24001.	0.7	12

#	Article	IF	CITATIONS
127	Electronic Structure, Mechanical and Magnetic Properties of the Quaternary Perovskites CaA3V4O12 (A = Mn, Fe, Co, Ni and Cu). Journal of Electronic Materials, 2020, 49, 1230-1242.	1.0	12
128	Ultraviolet spectroscopy of Pr+3 and its use in making ultraviolet filters. Current Applied Physics, 2009, 9, 234-237.	1.1	11
129	Electron penetration depth in amorphous AlN exploiting the luminescence of AlN:Tm/AlN:Ho bilayers. Current Applied Physics, 2009, 9, 417-421.	1.1	11
130	Pressure driven spin crossover and isostructural phase transition in LaFeO3. Journal of Applied Physics, 2013, 114, .	1.1	11
131	Electronic band structure of LaCoO3/Y/Mn compounds. Physica B: Condensed Matter, 2013, 410, 112-119.	1.3	11
132	Mechanical properties and variation in SOC going from La to Nd in intermetallic RIn3 and RSn3 (RÂ= La,) Tj ETQq	0 0 0 rgB⁻ 1.7 rgB⁻	T /Qyerlock 10
133	Comparative study of thermoelectric properties of Co based filled antimonide skutterudites with and without SOC effect. Computational Materials Science, 2017, 131, 308-314.	1.4	11
134	125 Te NMR shielding and optoelectronic spectra in XTe 3 O 8 (XÂ=ÂTi, Zr, Sn and Hf) compounds: Ab initio calculations. Journal of Molecular Structure, 2017, 1148, 223-230.	1.8	11
135	First principle studies of structural, magnetic and elastic properties of orthorhombic rare-earth diaurides intermetallics RAu2 (R=La, Ce, Pr and Eu). Materials Chemistry and Physics, 2018, 212, 44-50.	2.0	11
136	Theoretical studies of CsSnX3 (X = Cl, Br and I) for energy storage and hybrid solar cell applications. Materials Today Communications, 2020, 25, 101517.	0.9	11
137	Spin-orbit coupling effect on the optoelectronic and thermoelectric properties of the perovskites A3SnO (A = Ca, Sr and Ba). Materials Science in Semiconductor Processing, 2021, 132, 105905.	1.9	11
138	Spectroscopy of gadolinium ion and disadvantages of gadolinium impurity in tissue compensators and collimators, used in radiation treatment planning. Spectroscopy, 2007, 21, 205-210.	0.8	10
139	Interferences in photodetachment of a triatomic negative ion. Applied Physics Letters, 2009, 94, 041125.	1.5	10
140	Superluminal propagation in a poly-chromatically driven gain assisted four-level N-type atomic system. Physica Scripta, 2013, 88, 045402.	1.2	10
141	Density functional studies of magneto-optic properties of CdCoS. Journal of Magnetism and Magnetic Materials, 2014, 351, 60-64.	1.0	10
142	The effect of Kerr nonlinearity and Doppler broadening on slow light propagation. Laser Physics, 2014, 24, 025201.	0.6	10
143	Electronic structure of the LiAA′O6 (AÂ=ÂNb, Ta, and A′Â=ÂW, Mo) ceramics by modified Becke-Johnson potential. Optical Materials, 2016, 58, 466-475.	1.7	10
144	127I NMR calculations in binary metal iodides by PBE-GGA, YS-PBEO and mBJ exchange correlation potentials. Solid State Nuclear Magnetic Resonance, 2017, 82-83, 10-15.	1.5	10

#	Article	IF	CITATIONS
145	Effects of chemical potential on the thermoelectric performance of alkaline-earth based skutterudites (AFe4Sb12, A Ca, Sr and Ba). Journal of Alloys and Compounds, 2017, 694, 253-260.	2.8	10
146	DFT study on thermo-elastic properties of Ru2FeZ (Z = Si, Ge, Sn) Heusler alloys. International Journal of Modern Physics B, 2018, 32, 1850045.	1.0	10
147	Spatio-temporal variations of absorbing aerosols and their relationship with meteorology over four high altitude sites in glaciated region of Pakistan. Journal of Atmospheric and Solar-Terrestrial Physics, 2019, 190, 84-95.	0.6	10
148	First-principles investigation on electronic structure, magnetic states and optical properties of Mn-doped SnS2 monolayer via strain engineering. Physica E: Low-Dimensional Systems and Nanostructures, 2021, 134, 114842.	1.3	10
149	Classification of partially reflecting surfaces using photodetached electron spectrum. International Journal of Quantum Chemistry, 2011, 111, 4067-4071.	1.0	9
150	Robust halfâ€metallicity of AlCoN and AlNiN. International Journal of Quantum Chemistry, 2012, 112, 2668-2674.	1.0	9
151	Control of Wave Propagation and Effect of Kerr Nonlinearity on Group Index. Communications in Theoretical Physics, 2013, 60, 87-92.	1.1	9
152	Comparison of band profiles and magnetic properties of the different phases of BaTbO3. Computational Materials Science, 2013, 67, 151-155.	1.4	9
153	Conductivity dependent surface plasmon polariton propagation. Laser Physics, 2016, 26, 095204.	0.6	9
154	Strongly correlated intermetallic rare-earth monoaurides (Ln-Au): Ab-initio study. Journal of Rare Earths, 2018, 36, 1106-1111.	2.5	9
155	Unusual refraction and Fizeau effect for a linearly polarized pulse in rotary chiral media. Journal of the Optical Society of America B: Optical Physics, 2018, 35, 1817.	0.9	9
156	Cross-Kerr nonlinearity in the surface plasmon polariton waves generated at the interface of graphene and gain medium. Europhysics Letters, 2018, 122, 57003.	0.7	9
157	Physical properties and possible applications of gold-based rare earth intermetallics (R-Au): A review. Journal of Magnetism and Magnetic Materials, 2019, 490, 165477.	1.0	9
158	Tuning the Properties of Novel Magnetic Oxide via Co–Bi Co-substitution Including Theoretical Background of Characterization Techniques. Journal of Superconductivity and Novel Magnetism, 2021, 34, 2313-2329.	0.8	9
159	Growth evolution of high-quality MOCVD aluminum nitride using nitrogen as carrier gas on the sapphire substrate. Journal of Materials Research, 2021, 36, 4360-4369.	1.2	9
160	Selective sensing of NH3 and CH2O molecules by novel 2D porous hexagonal boron oxide (B3O3) monolayer: A DFT approach. Surfaces and Interfaces, 2022, 29, 101767.	1.5	9
161	Luminescence from Cr^+3-doped AlN films deposited on optical fiber and silicon substrates for use as waveguides and laser cavities. Applied Optics, 2010, 49, 653.	2.1	8
162	Structural, electronical and thermoelectric properties of CdGa2S4 compound under high pressures by mBJ approach. Journal of Materials Science: Materials in Electronics, 2017, 28, 16476-16483.	1.1	8

#	Article	IF	CITATIONS
163	Highâ€Temperature Operation of Al <sub><i>x</i></sub> Ga <sub>1â<sup>^</sup><i>x</i></sub> N ( <i>x</i> > 0.4 Channel Metal Oxide Semiconductor Heterostructure Field Effect Transistors with Highâ€ <i>k</i> Atomic Layer Deposited Gate Oxides. Physica Status Solidi (A) Applications and Materials Science, 2020, 217, 1900802.	·) 0.8	8
164	Magneto-optical rotation of surface plasmon polaritons. Journal Physics D: Applied Physics, 2021, 54, 175107.	1.3	8
165	Control of surface plasmon-polaritons at interfaces between triple quantum dots and nanocomposites. Journal of Optics (United Kingdom), 2020, 22, 115002.	1.0	8
166	Strain effect on the electronic and photocatalytic properties of GaN-MSSe (M=Mo, W). Journal of Solid State Chemistry, 2022, 306, 122798.	1.4	8
167	Pseudomorphic Al <sub>x</sub> Ga <sub>1â€x</sub> N MQW based deep ultraviolet light emitting diodes over sapphire. Physica Status Solidi C: Current Topics in Solid State Physics, 2014, 11, 798-801.	0.8	7
168	Investigation of the optical properties of P, As and Sb incorporated AlGaX alloys using full potential linearized augmented plane wave method. Computer Physics Communications, 2014, 185, 2829-2833.	3.0	7
169	Temporal cloak via Doppler broadening. Laser Physics, 2015, 25, 065405.	0.6	7
170	Electric field gradient analysis of RIn 3 and RSn 3 compounds (R = La, Ce, Pr and Nd). Intermetallics, 2017, 91, 95-99.	1.8	7
171	Theoretical investigation of thermoelectric and elastic properties of intermetallic compounds ScTM (TM = Cu, Ag, Au and Pd). International Journal of Modern Physics B, 2018, 32, 1850004.	1.0	7
172	First principles studies of CsLnCdTe3 (LnÂ= Gdâ^'Tm) for green energy resources. Computational Condensed Matter, 2019, 21, e00427.	0.9	7
173	Enhanced and highly tunable Goos-Hächan shifts at a nanocomposite-graphene interface. Applied Physics Letters, 2019, 114, 161902.	1.5	7
174	The effect of potassium insertion on optoelectronic properties of cadmium chalcogenides. Materials Science in Semiconductor Processing, 2021, 122, 105466.	1.9	7
175	Intriguing electronic, optical and photocatalytic performance of BSe, M2CO2 monolayers and BSe–M2CO2 (M = Ti, Zr, Hf) van der Waals heterostructures. RSC Advances, 2021, 12, 42-52.	1.7	7
176	Investigation of Linear Tetra-Atomic Negative Ion by Photodetached-Electron Spectra. Chinese Physics Letters, 2011, 28, 083301.	1.3	6
177	Atom Microscopy via Dual Resonant Superposition. Communications in Theoretical Physics, 2015, 64, 741-746.	1.1	6
178	First-principle studies of the ternary palladates CaPd3O4 and SrPd3O4. Bulletin of Materials Science, 2016, 39, 1861-1870.	0.8	6
179	First-principles studies of pure and fluorine substituted alanines. International Journal of Modern Physics B, 2016, 30, 1650079.	1.0	6
180	Exergy analysis and optimisation of naphtha reforming process with uncertainty. International Journal of Exergy, 2018, 26, 247.	0.2	6

#	Article	IF	CITATIONS
181	Theoretical investigations of thermoelectric phenomena in binary semiconducting skutterudites. RSC Advances, 2019, 9, 24981-24986.	1.7	6
182	A computational study on the characteristics of open-shell H-bonding interaction between carbamic acid (NH2COOH) and HO2, HOS or HSO radicals. Journal of Molecular Modeling, 2019, 25, 189.	0.8	6
183	Electronic and optical properties of group IIA-IVB cubic perovskite oxides: Improved TB-mBJ study. Chemical Physics Letters, 2020, 757, 137887.	1.2	6
184	Intriguing electronic structure and photocatalytic performance of blueP–SMSe and blueP–SeMS (M =) Tj ETQ	9q0 0 0 rgl 1.7	BT <sub>6</sub> /Overlock
185	Investigation of the Goos-HÃ <b>¤</b> chen shift in an optomechanical cavity via quantum control. Physical Review A, 2020, 102, .	1.0	6
186	Irradiation effects on Nd and W doped Aluminum Nitride thin films. Physica B: Condensed Matter, 2020, 586, 412086.	1.3	6
187	Response of structural and optical properties against proton irradiation in AlN:Tm thin films. Radiation Physics and Chemistry, 2021, 180, 109234.	1.4	6
188	Coherent control of surface plasmon polariton via spontaneously generated coherence. European Physical Journal Plus, 2021, 136, 1.	1.2	6
189	Interferences in Photodetached Electron Spectra from a Linear Tetra-Atomic Negative Ion. Chinese Physics Letters, 2011, 28, 063301.	1.3	6
190	Magneto-electronic studies of the inverse-perovskite (Eu3O)In. Journal of Magnetism and Magnetic Materials, 2015, 381, 34-40.	1.0	5
191	Structural, Mechanical and Optoelectronic Properties of Y2M2O7 (M = Ti, V and Nb) Pyrochlores: A First Principles Study. Journal of Electronic Materials, 2017, 46, 4640-4648.	1.0	5
192	Electron correlation and spin-orbit coupling effects in scandium intermetallic compounds ScTM (TM) Tj ETQq0 0 (	D rgBT /Ov	erlock 10 Tf

193	Theoretical studies of cubic AuCu3-type intermetallic actinide compounds NpPx3 (Px=Al, Ga, In). Intermetallics, 2018, 93, 77-84.	1.8	5
194	Electronic structure and magnetic properties of the quaternary perovskites LnMn <sub>3</sub> V <sub>4</sub> O <sub>12</sub> (Ln = La, Nd and Gd). Philosophical Magazine, 202 100, 2386-2401.	200.7	5
195	Investigation of MOCVD grown crack-free 4Âμm thick aluminum nitride using nitrogen as a carrier gas. MRS Advances, 2021, 6, 456-460.	0.5	5
196	Al-decorated C24N24 fullerene: A robust single-atom catalyst for CO oxidation. Polyhedron, 2021, , 115497.	1.0	5
197	Luminescence Enhancement in Amorphous AlN:W by Co-Doped Gd+3. IEEE Photonics Technology Letters, 2015, 27, 1519-1522.	1.3	4
198	DFT and post-DFT studies of metallic MXY3-type compounds for low temperature TE applications. Solid State Communications, 2016, 243, 28-35.	0.9	4

#	Article	IF	CITATIONS
199	Role of the Crystal Lattice Constants and Band Structures in the Optoelectronic Spectra of CdGa <sub>2</sub> S <sub>4</sub> by DFT Approaches. Zeitschrift Fur Anorganische Und Allgemeine Chemie, 2017, 643, 839-849.	0.6	4
200	First-Principles Study of Electronic Structure, Mechanical, and Thermoelectric Properties of Ternary Palladates CdPd3O4 and TlPd3O4. Journal of Electronic Materials, 2018, 47, 1871-1880.	1.0	4
201	Theoretical studies of the electronic structure and magnetic properties of aluminum-rich intermetallic alloy Al13Fe <sub>4</sub> . International Journal of Modern Physics B, 2018, 32, 1850201.	1.0	4
202	Computational Study of Ru <sub>2</sub> TiZ (Z = Si, Ge, Sn) for Structural, Mechanical and Vibrational Properties. Zeitschrift Fur Naturforschung - Section A Journal of Physical Sciences, 2019, 74, 545-550.	0.7	4
203	Incoherent and coherent manipulation of surface plasmon hole burning. Laser Physics Letters, 2019, 16, 036001.	0.6	4
204	RemovalÂof nitrous and carbon mono oxideÂfrom flue gasesÂby Si-coordinated nitrogen doped C60-fullerene: A DFT approach. Molecular Catalysis, 2021, 509, 111674.	1.0	4
205	Structural and optoelectronic properties of CsLnZnTe3 (LnÂ= La, Pr, Nd and Sm). Journal of Rare Earths, 2023, 41, 388-396.	2.5	4
206	Diffusion of Six-Atom Cu Islands on Cu(111) and Ag(111). Chinese Physics Letters, 2011, 28, 053601.	1.3	3
207	Structural Analysis and Infrared Emission from Ti+3 Doped AlN Deposited on Si(100) and Si(111) Substrates and Optical Fibers. Journal of Low Temperature Physics, 2015, 179, 365-374.	0.6	3
208	Spectral Hole Burning via Kerr Nonlinearity. Communications in Theoretical Physics, 2015, 64, 473-478.	1.1	3
209	Time gap for temporal cloak based on spectral hole burning in atomic medium. Chinese Physics B, 2016, 25, 084205.	0.7	3
210	Cavity electromagnetically induced transparency via spontaneously generated coherence. Journal of Modern Optics, 2017, 64, 1777-1783.	0.6	3
211	Electronic and Magnetic Structures, Magnetic Hyperfine Fields and Electric Field Gradients in UX3 (XÂ=ÂIn, Tl, Pb) Intermetallic Compounds. Journal of Electronic Materials, 2018, 47, 1045-1058.	1.0	3
212	Control of the Faraday rotation via electromagnetically induced transparency medium and graphene metasurfaces. Journal of Optics (United Kingdom), 2019, 21, 105401.	1.0	3
213	Structural, electrical and optical characterizations of yttrium doped aluminum nitride thin films before and after ions irradiation. Optical Materials, 2021, 116, 111097.	1.7	3
214	Silicon-doped boron nitride graphyne-like sheet for catalytic N2O reduction: A DFT study. Journal of Molecular Graphics and Modelling, 2022, 114, 108186.	1.3	3
215	Robust Half-Metallicity in a Chromium-Substituted AlN. Chinese Physics Letters, 2011, 28, 108501.	1.3	2
216	Structural, Thermal and Luminescence Properties of AlN:Tm Thin Films Deposited on Silicon Substrate and Optical Fiber. Semiconductors, 2018, 52, 2039-2045.	0.2	2

#	Article	IF	CITATIONS
217	Synergetic Effect of Calcium Doping on Catalytic Activity of Manganese Ferrite: DFT Study and Oxidation of Hydrocarbon. Crystals, 2020, 10, 335.	1.0	2

## 218 Enhanced cross-Kerr nonlinearity induced PT -symmetry in optical lattices. Journal of Optics (United) Tj ETQq0 0 QrgBT /Overlock 10 T

219	Coherent Surface Plasmon Hole Burning via Spontaneously Generated Coherence. Molecules, 2021, 26, 6497.	1.7	2
220	Co Anchored B 36 Cluster as a Novel Single Atom Catalyst for Removing Toxic CO Molecules: A Mechanistic Firstâ€Principles Study. ChemistrySelect, 2022, 7, .	0.7	2
221	Revealing the quasiparticle electronic and excitonic nature in cubic, tetragonal, and hexagonal phases of FAPbI <sub>3</sub> . AIP Advances, 2022, 12, 025330.	0.6	2
222	Photodetachment of a Homo-Nuclear Linear Tetra-Atomic Negative Molecular Ion. Chinese Physics Letters, 2012, 29, 043301.	1.3	1
223	Structural, Mechanical and Magneto-Electronic Properties of the Ternary Sodium Palladium and Platinum Oxides. Zeitschrift Fur Naturforschung - Section A Journal of Physical Sciences, 2015, 70, 815-822.	0.7	1
224	The Influence of Oxygen Substitution on the Optoelectronic Properties of ZnTe. Journal of Chemistry, 2016, 2016, 1-8.	0.9	1
225	Controlling Casimir force via coherent driving field. European Physical Journal D, 2016, 70, 1.	0.6	1
226	Virtual sensing of catalytic naphtha reforming process under uncertain feed conditions. , 2018, , .		1
227	Predictions of bandgap and subbands of γâ~ Al2O3 in presence of intrinsic point defects by DFT+TB-mBJ. Computational Condensed Matter, 2019, 19, e00379.	0.9	1
228	Electronic structure and magnetic properties of the Mg-rich intermetallic NdNiMg5 by hybrid density functional theory. Intermetallics, 2020, 127, 106969.	1.8	1
229	Fabrication and Ions Irradiation Study of AlN:Gd Thin Films. ECS Journal of Solid State Science and Technology, 2022, 11, 043002.	0.9	1
230	Thermoelectric, optoelectronic and magnetic properties of BaLn2ZnO5 (LnÂ=ÂEu, Pr, Sm) insulators by GGA/mBJÂ+ÂU exchange-correlation approaches. Materials Science and Engineering B: Solid-State Materials for Advanced Technology, 2022, 283, 115772.	1.7	1
231	The influence of Sr and Fe on the conductance of magnetoresistant compounds. Russian Journal of Physical Chemistry A, 2008, 82, 2169-2172.	0.1	0
232	Study of robust half-metallicity of Ga0.875Cr0.125As. Indian Journal of Physics, 2014, 88, 385-389.	0.9	0
233	Superposition of Stationary Wave Fields Via Atom Microscopy. Communications in Theoretical Physics, 2015, 63, 340-346.	1.1	0
234	Hyperfine field, electric field gradient, quadrupole coupling constant and magnetic properties of challenging actinide digallide. Physica B: Condensed Matter, 2017, 526, 102-109.	1.3	0

#	Article	IF	CITATIONS
235	Enhanced dispersive properties of graphene plasmons on substrates of composite materials. Journal of Optics (United Kingdom), 2021, 23, 055001.	1.0	ο
236	Optical activity and excitation of surface plasmon polaritons with electromagnetically induced chiral media. Journal of the Optical Society of America B: Optical Physics, 2020, 37, 2936.	0.9	0